Title: Protocerebral bridge neurons that regulate sleep in *Drosophila melanogaster*

Authors: Jun Tomita[1]*, Gosuke Ban[1]*, Yoshiaki S. Kato[1], and Kazuhiko Kume[1,2]

1. Department of Neuropharmacology, Graduate School of Pharmaceutical Sciences, Nagoya City University, Nagoya 467-8603, Japan

2. Corresponding author: Department of Neuropharmacology, Graduate School of Pharmaceutical Sciences, Nagoya City University, 3-1 Tanabe, Mizuho, Nagoya 467-8603, Japan.

Tel/Fax., +81-52-836-3676. Email, kume@phar.nagoya-cu.ac.jp

*These authors contributed equally to this work.

Abstract

The central complex is one of the major brain regions that control sleep in *Drosophila*, but the circuitry details of sleep regulation have yet to be elucidated. Here, we show a novel sleep-regulating neuronal circuit in the protocerebral bridge (PB) of the central complex. Activation of the PB interneurons labeled by the *R59E08-Gal4* and the PB columnar neurons in the *R52B10-Gal4* promoted sleep and wakefulness, respectively. A targeted GFP reconstitution across synaptic partners (t-GRASP) analysis demonstrated synaptic contacts between these two groups of sleep-regulating PB neurons. Furthermore, we found that activation of a pair of dopaminergic (DA) neurons projecting to the PB (T1 DA neurons) decreased sleep. The wake-promoting T1 DA neurons and the sleep-promoting PB interneurons formed close associations. *Dopamine 2-like receptor* (*Dop2R*) knockdown in the sleep-promoting PB interneurons increased sleep. These results indicated that the neuronal circuit in the PB regulated by dopamine signaling mediates sleep-wakefulness.

Introduction

Sleep is a basic physiological state evolutionarily conserved among animal species (Allada and Siegel, 2008; Cirelli and Tononi, 2008). The fruit fly, *Drosophila melanogaster*, has emerged as a powerful model system for uncovering the molecular and cellular basis of sleep-wakefulness. Sleep in *Drosophila* is defined by behavioral features including circadian control of the timing of sleep, homeostasis of the amount of sleep and increased arousal threshold as in other animal species that do not exhibit the characteristic electroencephalogram patterns of sleep (Campbell and Tobler, 1984).

The central complex is a unique midline neuropil structures in the adult insect brain, composed of four substructures, the protocerebral bridge (PB), the fan-shaped body (FB), the ellipsoid body (EB) and the noduli (NO), and serves as a higher-order integrator for sensory information and various motor control (Homberg, 2008). Accumulating evidence from a number of neurogenetic studies has established a crucial role for the central complex in *Drosophila* sleep regulation. The sleep-promoting neurons having extensive presynaptic arborizations in the dorsal layer of the FB (dFB) has been identified (Donlea et al., 2011; Ueno et al., 2012). Dopamine is a neurotransmitter that is essential for maintaining wakefulness in *Drosophila*, similar to mammals (Andretic et al., 2005; Kume et al., 2005). The protocerebral posterior medial 3 (PPM3) cluster of dopaminergic (DA) neurons projecting to the dFB neurons controls sleep through Dopamine 1-like receptor 1 (Dop1R1) signaling (Liu et al., 2012; Ueno et al., 2012). Neurons that project to the ventral layer of the FB promote sleep and mediate consolidation of long-term memory (Dag et al., 2019). Homeostatic mechanism of sleep would be associated with changes in neuronal activity of the sleep-promoting dFB neurons and their functional upstream neurons, the R5 neurons in the EB (Donlea et al., 2014; Liu et al., 2016). In addition, the dFB neurons form a recurrent circuit with the EB R5 neurons via helicon cells to regulate sleep homeostasis (Donlea et al., 2018). Regarding circadian regulation of sleep-wakefulness, recent studies have shown that sleep-modulating dorsal neurons 1 (DN1) of circadian clock neurons and EB ring neuron subtypes are functionally connected via sleep-promoting tubercular-bulbar (TuBu) neurons and that this circuit is likely to regulate sleep-wakefulness (Guo et al., 2018; Lamaze et al., 2018). Besides, sleep-promoting lateral posterior neurons (LPNs), another group of clock neurons, appear to form close associations to the sleep-promoting dFB neurons and activate these neurons (Ni et al., 2019). Detailed mechanisms for regulating sleep-wakefulness by the central complex are being clarified. However, because the four substructures of the central complex are interconnected, a population of central complex neurons other than the FB neurons and

55 the EB R5 neurons should also be implicated in the control of sleep-wakefulness.

56 Here, we begin to explore a novel sleep-regulating neuron in the central complex and discover
57 that the sleep-promoting PB interneurons have direct neuronal connections to the wake-promoting
58 PB columnar neurons projecting from the PB to the FB and the NO. Moreover, we reveal that T1
59 cluster of DA neurons regulates sleep by acting on the sleep-promoting PB interneurons through D2
60 dopamine receptor signaling.

Results

The PB defective mutant flies, *nob*^{KS49} decreased sleep

In order to examine the role of the central complex in sleep regulation, we tested eleven mutant strains with morphological defects in the central complex. These mutant flies were isolated histologically following ethyl methanesulfonate mutagenesis, except for *agn*^{X1}, which was isolated from a wild population (Strauss and Heisenberg, 1993). Flies were entrained to 12 h light : 12 h dark (LD) cycles for at least 3 days, then maintained in constant dark (DD) conditions. Locomotor activity was recorded in both LD and DD conditions. Sleep was defined as periods of immobile state lasting 5 min or longer, as previously described (Hendricks et al., 2000; Shaw et al., 2000; Huber et al., 2004; Kume et al., 2005). Because most of these structural mutants are still uncharacterized, their total daily activity and sleep were compared to those of three control strains (Canton-S (CS), *y w* and *w*^{1118}) under DD conditions. There were no significant differences in total daily activity and sleep between the three control strains (*Figure 1A,B*). Among the central complex mutants tested, *nob*^{KS49} flies showed significant hyperactivity compared with two control lines (CS and *y w*). *nob*^{KS49} mutants have a defect in the central part of PB (Strauss et al., 1992). No difference was seen in waking activity index, defined as total daily activity divided by the active period length, between *nob*^{KS49} and controls (*Figure 1C*), suggesting hyperactivity in *nob*^{KS49} flies is not attributed to aberrant locomotion. On average, total daily activity significantly increased by about 2-fold in *nob*^{KS49} relative to controls (*Figure 1A*). In contrast, total daily sleep of *nob*^{KS49} flies decreased to approximately half of that of the CS and *y w* controls (*Figure 1B*). These results suggest that PB is involved in sleep regulation.

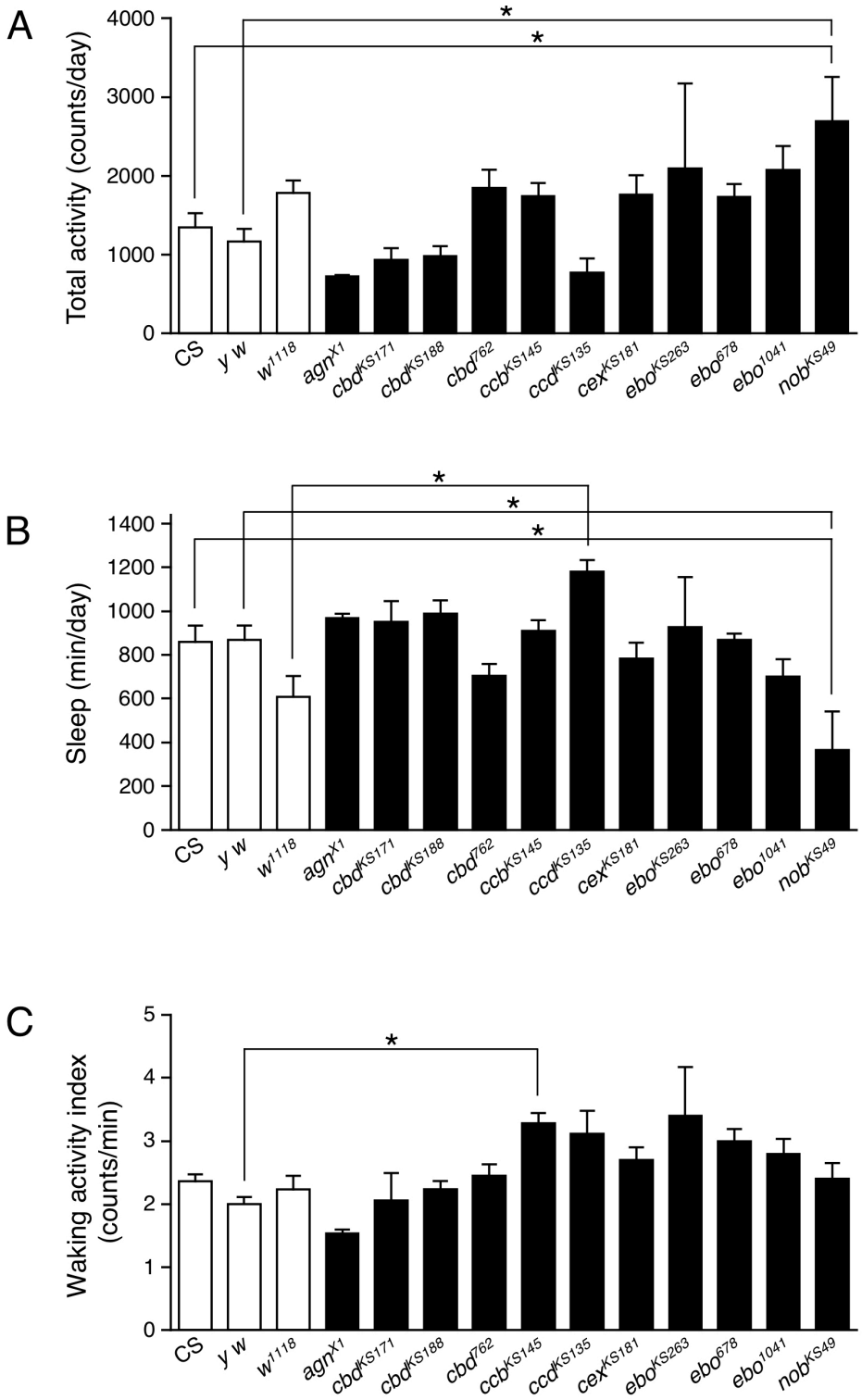

Figure 1. The PB defective *nob*^{KS49} decreased sleep.

Total daily activity **(A)**, total sleep **(B)** and waking activity index **(C)** for control flies (Canton-S, *y w* and w^{1118}, white bars) and mutant strains with structural defects in the central complex (black bars) in constant dark (DD) conditions. Data are averaged for 3 days and are presented as mean ± standard error of the mean (SEM) (n = 3-11 for each group). Groups with asterisks indicate statistically significant differences (Tukey-Kramer HSD test for normally distributed data, $p < 0.05$).

87 **Activation of *Gal4*-expressing neurons in *Gal4* drivers that express in the PB affected sleep**
88 To further explore the involvement of PB neurons in sleep regulation, we examined the effects of
89 transient thermogenetic activation of a subset of PB neurons using the temperature-sensitive cation
90 channel dTrpA1 on the amount of sleep. For this, fourteen *Gal4* driver lines that express strongly
91 in PB neurons (*PB-Gal4*) were selected from the Gal4 image data of the FlyLight Image Database
92 (https://flweb.janelia.org/cgi-bin/flew.cgi, Jenett et al., 2012). Progenies from the control (*PB-Gal4*
93 × w^{1118}) and the experimental (*PB-Gal4* × *UAS-dTrpA1*) crosses were grown at 22ºC to adulthood.
94 Sleep was measured in adult progeny flies in DD following LD cycles. These flies were transferred
95 from 22ºC to 29ºC for 24 h to conditionally activate dTrpA1-expressing neurons and then returned to
96 22ºC. Of the 14 *PB-Gal4* drivers tested, the acute activation of neurons with the 9 *Gal4* drivers
97 significantly decreased sleep. In particular, the decrease in the sleep amount induced by activation
98 of neurons using the *R52B10-Gal4* was most remarkable and flies hardly slept during neuronal
99 activation as previously reported (*Figure 2A-C*) (Liu et al., 2016). Although clear homeostatic sleep
100 recovery (sleep rebound) after sleep loss by the thermogenetic activation using the *R52B10-Gal4* was
101 reported (Liu et al., 2016), such a clear sleep rebound was not observed in our experimental conditions
102 (*Figure 2B,C*). On the other hand, the activation of Gal4 expressing neurons in the 3 of 14 *PB-Gal4*
103 drivers significantly increased sleep (*Figure 2A*). The largest effect on sleep induction was caused
104 by the neuronal activation using the *R59E08-Gal4*. In this *Gal4* driver, the amount of sleep in the
105 experimental flies peaked in the middle of the subjective day at 29ºC and was maintained at the peak
106 level during neuronal activation (*Figure 2D*). Sleep amount in the experimental flies was
107 significantly reduced compared with that in the control flies after stopping the activation.
108 The expression patterns of the *R52B10-Gal4* or the *R59E08-Gal4* drivers in the adult brains were
109 visualized using *UAS-mCD8::GFP*. The wake-promoting *R52B10-Gal4* drove strong expression in
110 several cell types of columnar neurons named PFN projecting from the PB to the ventral part of the
111 FB and contralateral NO (*Figure 2F*, left panel) as shown in the FlyLight database (Jenett et al., 2012)
112 and the previous report (Buchanan et al., 2015). In addition to these central complex substructures,
113 some neurons in the anterior ventrolateral protocerebrum (AVLP) were also be seen as intense GFP
114 signals (*Figure 2F*, right panel). The thermogenetic activation using the *R52H12-Gal4* or the
115 *R83A10-Gal4* that express strongly in the AVLP neuropil (the FlyLight database, Jenett et al., 2012)
116 did not result in a marked decrease in the amount of sleep (*Figure 2-figure supplement 1*). The
117 sleep-promoting *R59E08-Gal4* specifically labeled the PB strongly in the central complex (*Figure*
118 *2G*). These PB neurons were identified as PB interneurons according to their previously described

119 morphological features (Lin et al., 2013; Wolff et al., 2015). In addition, the ubiquitous strong
120 expression of GFP in the medulla cells was also detected in the *R59E08-Gal4* driver. Neuronal
121 activation using two *Gal4* drivers (*R14F09-Gal4* and *R59A12-Gal4*), whose expression patterns in
122 the medulla resemble that of the *R59E08-Gal4* (the FlyLight database, Jenett et al., 2012), did not
123 significantly increase the amount of sleep (*Figure 2-figure supplement 2*).

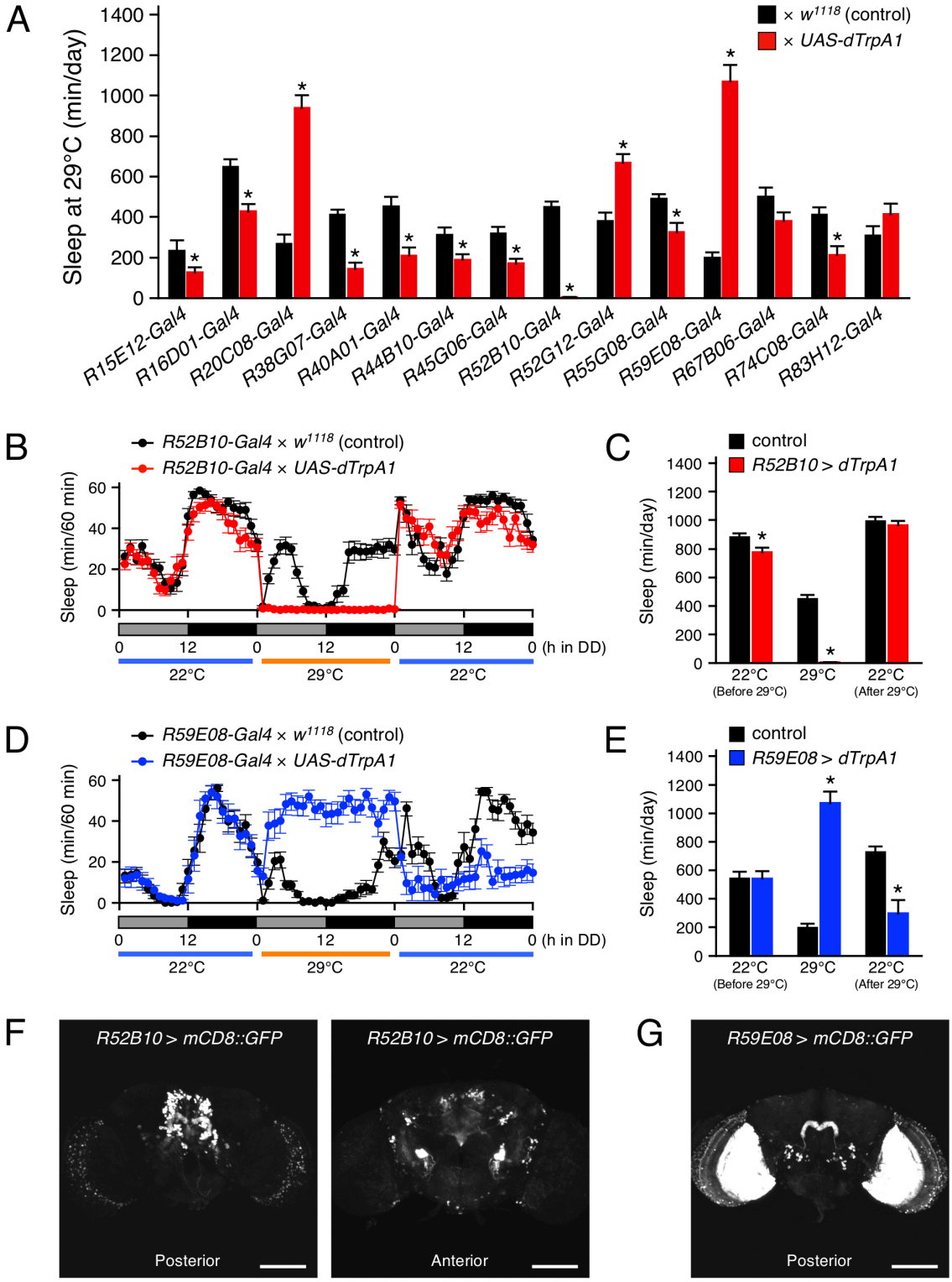

Figure 2. Acute activation of the PB neurons affected sleep.

(A) The amount of sleep per day at 29ºC in DD conditions in control flies (black bars) and flies expressing *dTrpA1* transgene by indicated *Gal4* drivers that highly express in PB neurons (red bars). For controls, each *Gal4* driver was crossed with w^{1118} (the genetic background of *UAS-dTrpA1* carrying flies). Data are presented as mean ± SEM (n = 6-16 for each group). Asterisks indicate statistically significant differences from control determined by a t-test ($p < 0.05$). **(B,C)** Sleep profiles for 60-min intervals (B) or total daily sleep (C) for controls (*R52B10-Gal4* × w^{1118}, black circles or bars, n = 16) or flies expressing *dTrpA1* with *R52B10-Gal4* (*R52B10-Gal4* × *UAS-dTrpA1*, red circles or bars, n = 16) in DD. Behavior was monitored in DD for 1 day at 22ºC, followed by 1 day at 29ºC (dTrpA1 activation), and 1 day at 22ºC. Gray and black bars under the horizontal axis indicate subjective day and night, respectively. Data are presented as mean ± SEM. *$p < 0.05$ vs. control; t-test. **(D,E)** Sleep profiles for 60-min intervals (D) or total daily sleep (E) for controls (*R59E08-Gal4* × w^{1118}, black circles or bars, n = 16) or flies expressing *dTrpA1* with *R59E08-Gal4* (*R59E08-Gal4* × *UAS-dTrpA1*, blue circles or bars, n = 10) in DD. Data are presented as mean ± SEM. *$p < 0.05$ vs. control; t-test. **(F,G)** Maximum-intensity projection of the confocal brain images of *R52B10-Gal4* (F) or *R59E08-Gal4* (G) crossed to *UAS-mCD8::GFP* flies. The scale bars represent 100 μm.

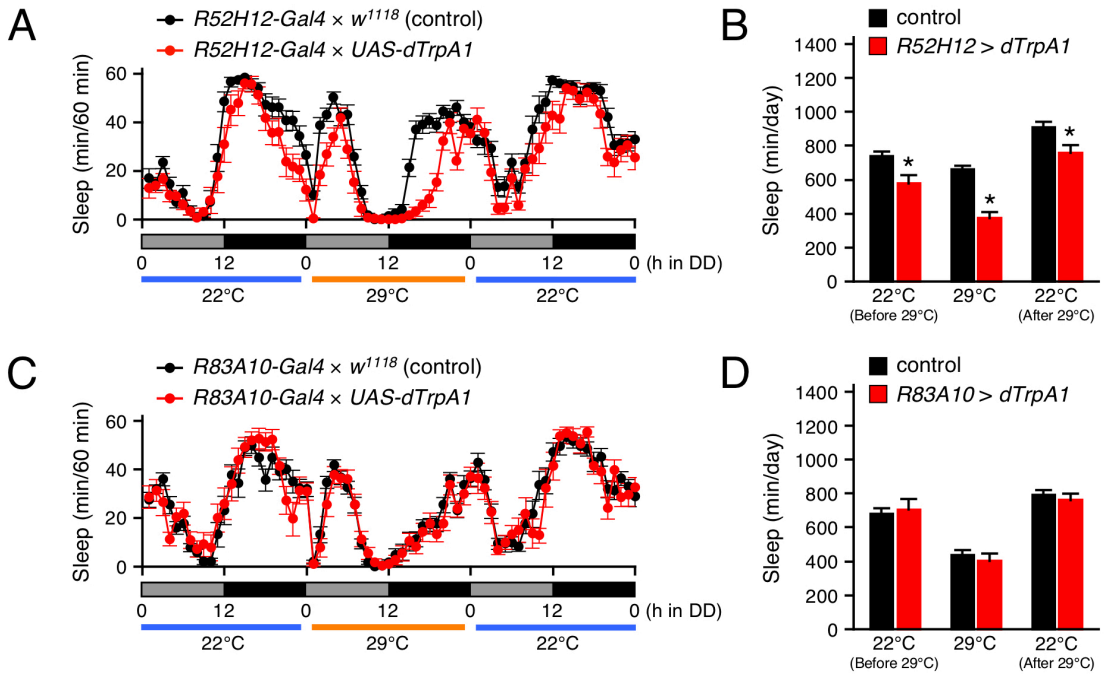

Figure 2-figure supplement 1. Neuronal activation using *Gal4* drivers that express in the AVLP did not remarkably decrease sleep.

(A,B) Sleep profiles for 60-min intervals (A) or total daily sleep (B) for controls (*R52H12-Gal4* × w^{1118}, black circles or bars, n = 16) or flies expressing *dTrpA1* with *R52H12-Gal4* (*R52H12-Gal4* × *UAS-dTrpA1*, red circles or bars, n = 14) in DD. The behavior was monitored as described in Figure 2. Data are presented as mean ± SEM. *$p < 0.05$ vs. control; t-test. **(C,D)** Sleep profiles for 60-

147 min intervals (C) or total daily sleep (D) for controls (*R83A10-Gal4* × w^{1118}, black circles or bars, *n*
148 = 16) or flies expressing *dTrpA1* with *R83A10-Gal4* (*R83A10-Gal4* × *UAS-dTrpA1*, red circles or
149 bars, *n* = 11) in DD. Data are presented as mean ± SEM.

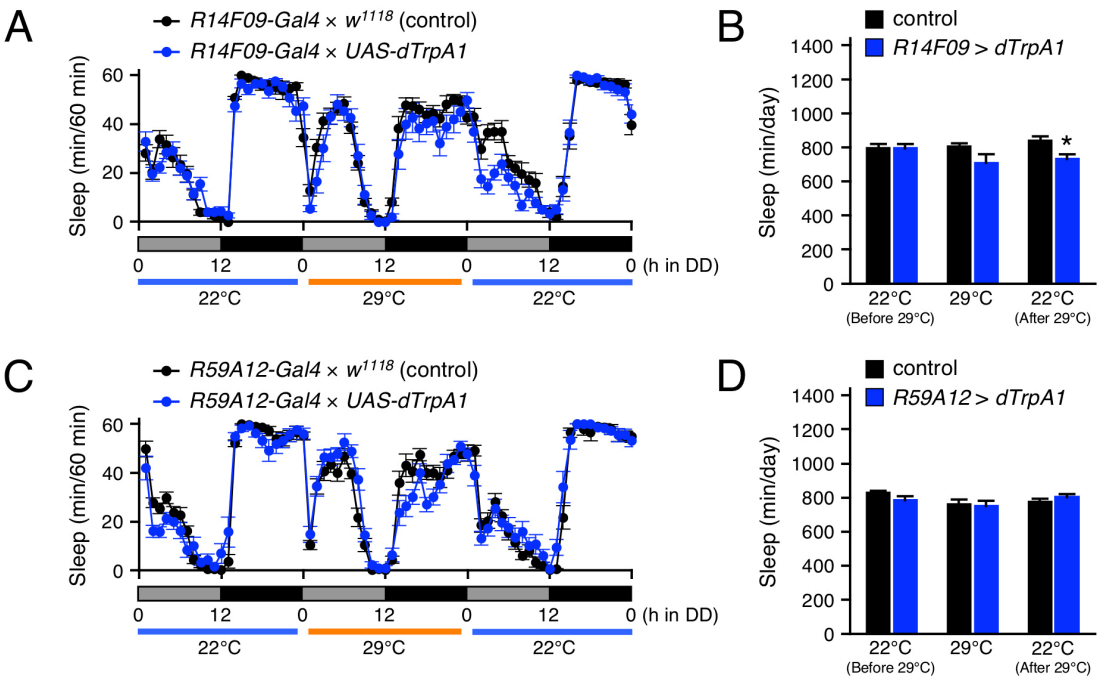

150 **Figure 2-figure supplement 2. Neuronal activation using *Gal4* drivers that express in the**
151 **medulla cells did not increase sleep.** **(A,B)** Sleep profiles for 60-min intervals (A) or total daily
152 sleep (B) for controls (*R14F09-Gal4* × w^{1118}, black circles or bars, *n* = 16) or flies expressing *dTrpA1*
153 with *R14F09-Gal4* (*R14F09-Gal4* × *UAS-dTrpA1*, blue circles or bars, *n* = 16) in DD. The behavior
154 was monitored as described in Figure 2. Data are presented as mean ± SEM. *$p < 0.05$ vs. control;
155 *t*-test. **(C,D)** Sleep profiles for 60-min intervals (C) or total daily sleep (D) for controls (*R59A12-*
156 *Gal4* × w^{1118}, black circles or bars, *n* = 15) or flies expressing *dTrpA1* with *R59A12-Gal4* (*R59A12-*
157 *Gal4* × *UAS-dTrpA1*, blue circles or bars, *n* = 16) in DD. Data are presented as mean ± SEM.

158 **Activation of PB interneurons with *R59E08-Gal4* increased sleep**

159 The sleep-promoting *R59E08-Gal4* was expressed not only in the adult brain but also in the ventral
160 nerve cord (VNC) (*Figure 3A*). To determine which targeted neurons in this driver are responsible
161 for the sleep induction, we employed *tsh-Gal80*, which inhibits Gal4-mediated transcription in the
162 VNC. The incorporation of the *tsh-Gal80* transgene successfully blocked *R59E08-Gal4* induced
163 GFP expression in the VNC without affecting its expression pattern in the brain (*Figure 3A*).
164 Activation of *R59E08-Gal4*-expressing neurons with *tsh-Gal80* also markedly increased in the
165 amount of sleep, indicating that brain neurons labeled by *R59E08-Gal4* contribute dTrpA1-mediated
166 sleep induction (*Figure 3B,C* and *Figure 2D,E*). On the other hand, decreased sleep caused after
167 dTrpA1 activation was completely restored by introducing *tsh-Gal80*, indicating that *R59E08-Gal4*-
168 expressing the VNC neurons are involved in this sleep phenotype. Thus, distinct populations of
169 *R59E08-Gal4*-expressing neurons participate in the sleep phenotypes induced during or after dTrpA1
170 activation.

171 Because the DAM system only detects motions of a fly passing through an infrared beam that
172 bisects a glass tube at the center, continuing feeding or grooming away from the beam path are
173 detected as apparent inactivity (continuous bins with the value of zero). To confirm that the flies
174 certainly sleep by activation of *R59E08-Gal4*-expressing brain neurons, we performed video analysis
175 of the behavior of these flies in glass tubes during the late subjective-day (CT 8 to CT 12) at 29ºC
176 (*Figure 3D*). The temperature was shifted from 22ºC to 29ºC at CT 0. As expected from the sleep
177 patterns observed by the DAM system, the experimental flies (*R59E08-Gal4* × *tsh-Gal80*; *UAS-*
178 *dTrpA1*) displayed little locomotor activity compared to controls (*R59E08-Gal4* × *tsh-Gal80*). The
179 immobile flies did not show excessive feeding or grooming, and paralysis in naked-eye observation.

180 We also found that the sleep phenotypes induced during or after activation of *R59E08-Gal4*-
181 expressing neurons were largely rescued by introducing $Cha^{7.4kb}$-*Gal80* transgene, which prohibits
182 Gal4 activity in cholinergic neurons (*Figure 3E,F*). Taken together, these results indicate that the
183 PB interneurons labeled by *R59E08-Gal4* were sleep-promoting and were primarily cholinergic.

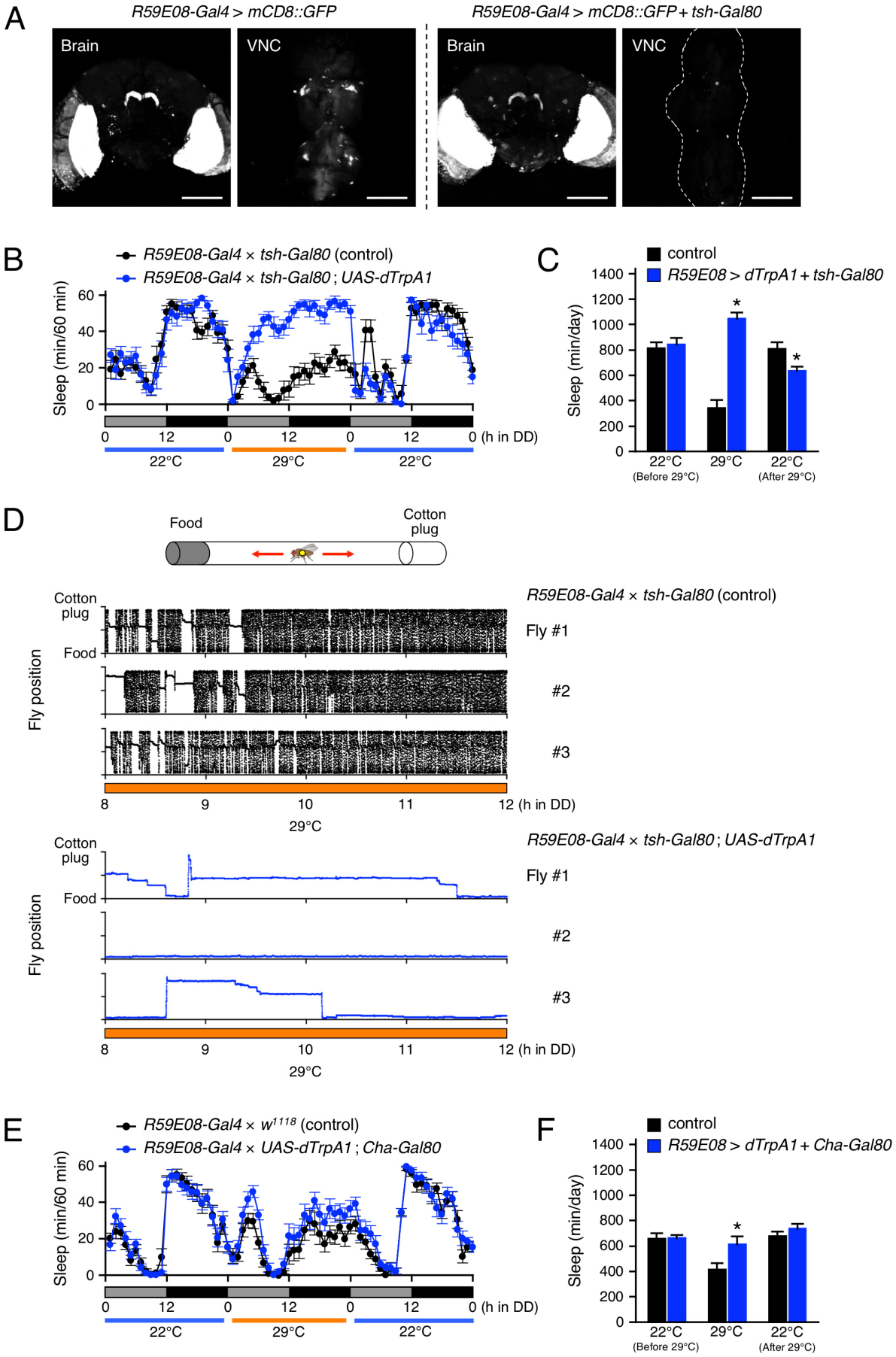
A
R59E08-Gal4 > mCD8::GFP
R59E08-Gal4 > mCD8::GFP + tsh-Gal80
Brain
VNC
Brain
VNC
B
R59E08-Gal4 × tsh-Gal80 (control)
R59E08-Gal4 × tsh-Gal80 ; UAS-dTrpA1
Sleep (min/60 min)
60
40
20
0
0
12
0
12
0
12
0 (h in DD)
22°C
29°C
22°C
C
control
R59E08 > dTrpA1 + tsh-Gal80
Sleep (min/day)
1400
1200
1000
800
600
400
200
0
*
*
22°C
(Before 29°C)
29°C
22°C
(After 29°C)
D
Food
Cotton plug
Cotton plug
Food
Fly position
R59E08-Gal4 × tsh-Gal80 (control)
Fly #1
#2
#3
8
9
10
11
12 (h in DD)
29°C
Cotton plug
Food
Fly position
R59E08-Gal4 × tsh-Gal80 ; UAS-dTrpA1
Fly #1
#2
#3
8
9
10
11
12 (h in DD)
29°C
E
R59E08-Gal4 × w1118 (control)
R59E08-Gal4 × UAS-dTrpA1 ; Cha-Gal80
Sleep (min/60 min)
60
40
20
0
0
12
0
12
0
12
0 (h in DD)
22°C
29°C
22°C
F
control
R59E08 > dTrpA1 + Cha-Gal80
Sleep (min/day)
1400
1200
1000
800
600
400
200
0
*
22°C
(Before 29°C)
29°C
22°C
(After 29°C)

184 **Figure 3. *R59E08-Gal4*-expressing PB interneurons promote sleep.**
185 **(A)** Maximum-intensity projection of the confocal brain or ventral nerve cord (VNC) images of flies
186 expressing *UAS-mCD8::GFP* under the control of *R59E08-Gal4* (left two panels) or *R59E08-Gal4*
187 with *tsh-Gal80* (right two panels). Transgene *tsh-Gal80* efficiently suppressed *R59E08-Gal4* driven
188 GFP expression in the VNC, while did not in the brains. The scale bars indicate 100 μm. **(B,C)**
189 Sleep profiles in 60-min intervals (B) or total daily sleep (C) for control flies (*R59E08-Gal4* × *tsh-*
190 *Gal80*, black circles or bars, n = 12) or flies expressing *dTrpA1* in *R59E08-Gal4* brain neurons
191 (*R59E08-Gal4* × *tsh-Gal80*; *UAS-dTrpA1*, blue circles or bars, n = 11) in DD. The behavior was
192 monitored as described in Figure 2. Data are presented as mean ± SEM. *$p < 0.05$ vs. control; *t*-
193 test. **(D)** Horizontal movements of the centroid of three representative control flies (*R59E08-Gal4*
194 × *tsh-Gal80*, black circles) or flies expressing *dTrpA1* in *R59E08-Gal4* brain neurons (*R59E08-Gal4*
195 × *tsh-Gal80*; *UAS-dTrpA1*, blue circles) in a glass tube at 29°C during the late subjective day (CT 8
196 to CT 12). Positions of the cotton plug and the food were at the top and the bottom in each plot,
197 respectively. The behavior of flies was recorded at 2 frames/sec using an infrared video camera in
198 DD conditions. The fly position in a glass tube was calculated for each image using an ImageJ
199 plugin. **(E,F)** Sleep profiles in 60-min intervals (E) or total daily sleep (F) for control flies (*R59E08-*
200 *Gal4* × w^{1118}, black circles or bars, n = 16) or flies expressing *dTrpA1* in *R59E08-Gal4* except
201 cholinergic neurons (*R59E08-Gal4* × *tsh-Gal80*; *UAS-dTrpA1*; $Cha^{7.4kb}$-*Gal80*, blue circles or bars,
202 n = 16) in DD. Data are presented as mean ± SEM. *$p < 0.05$ vs. control; *t*-test.

203 **PFN neurons were wake-promoting neurons**

204 As shown in *Figure 4A*, *tsh-Gal80* effectively attenuated the wake-promoting *R52B10-Gal4* driven
205 GFP expression in the VNC without effect on its expression in the brain. Activation of the brain
206 neurons targeted by *R52B10-Gal4* resulted in a dramatic reduction in the amount of sleep comparable
207 to that evoked by activating both the brain and the VNC neurons using this *Gal4* driver (*Figure 4B,C*
208 and *Figure 2B,C*). *Cha*$^{7.4kb}$*-Gal80* was able to fully revert the decreased sleep caused by activation
209 of *R52B10-Gal4*-expressing neurons (*Figure 4D,E* and *Figure 2B,C*). These results suggest that
210 cholinergic brain neurons labeled by *R52B10-Gal4* are wake-promoting.

211 Next, we searched for *R52B10-Gal4*-expressing brain neurons that contribute to the promotion of
212 wakefulness by a genetic mosaic approach. Using the mosaic analysis with a repressible cell marker
213 (MARCM) system, the *dTrpA1* and *GFP* were randomly co-expressed in a subpopulation of neurons
214 using *R52B10-Gal4* with FRT/FLP-induced mitotic recombination. We measured the amount of
215 sleep in these genetically mosaic flies at 22ºC and then 29ºC under DD conditions. The change in
216 sleep amount (ΔSleep) in individual flies was calculated by subtracting the amount of sleep during
217 the 12-h subjective night at 29ºC from that at 22ºC (*Figure 5A*). In this experiment, ΔSleep value
218 above the mean plus two times standard deviation (+2 SD) was regarded as a significant decrease in
219 subjective-night sleep at 29ºC. Of 133 flies examined, 7 flies had a ΔSleep value above the mean
220 +2 SD (426 min). After measuring the amount of sleep, the brains of these flies were dissected and
221 immunostained to determine GFP expression co-expressed with dTrpA1. GFP expression in the
222 flies with significantly reduced sleep labeled the PFN neurons in all but one of the flies shown in #7
223 in *Figure 5B*. By contrast, in the 7 individuals having ΔSleep value near the average, 2 flies were
224 labeled with the PFN neurons (#5 and #6 in *Figure 5C*), while the remaining flies were either not
225 labeled at all (#1 and #2) or labeled with neurons different from the PFN neurons (#3, #4, #7).

226 Moreover, to ensure that the PFN neurons labeled by *R52B10-Gal4* are the wake-promoting
227 neurons, we employed *c465-Gal4* that drives expression in these neurons participating in the tuning
228 of the magnitude of locomotor handedness (Buchanan et al., 2015). Because *c465-Gal4* is also
229 strongly expressed in the mushroom bodies that is another brain neuropil structures involved in
230 *Drosophila* sleep regulation (Joiner et al., 2006; Pitman et al., 2006; Sitaraman et al., 2015a), we used
231 *MB247-Gal80*, which blocks the activity of Gal4 in the mushroom bodies (*Figure 5D*). As expected,
232 activation of *c465-Gal4*-expressing neurons except for mushroom body neurons significantly
233 decreased sleep, as did the activation of *R52B10-Gal4*-expressing neurons (*Figure 5E,F*). These
234 results indicate that the PFN neurons labeled by *R52B10-Gal4* are wake-promoting.

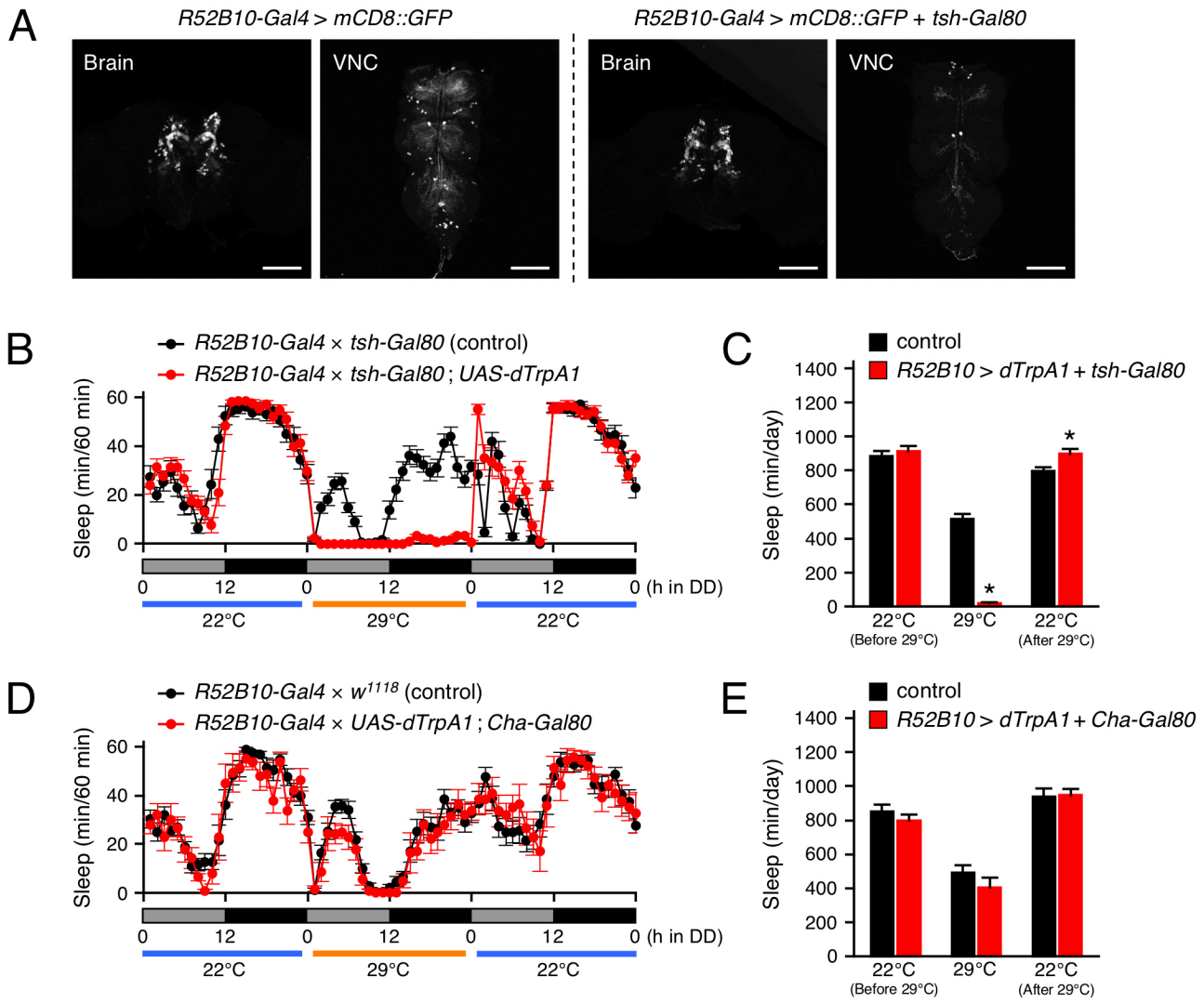

Figure 4. Activation of *R52B10-Gal4*-expressing cholinergic neurons in the brain promotes wakefulness.

(A) Maximum-intensity projection of the confocal brain or VNC images of flies expressing *UAS-mCD8::GFP* under the control of *R52B10-Gal4* (left two panels) or *R52B10-Gal4* with *tsh-Gal80* (right two panels). The *tsh-Gal80* efficiently suppressed *R52B10-Gal4* driven GFP expression in the VNC, while did not in the brains. **(B,C)** Sleep profiles in 60-min intervals (B) or total daily sleep (C) for control flies (*R52B10-Gal4* × *tsh-Gal80*, black circles or bars, $n = 16$) or flies expressing *dTrpA1* in *R52B10-Gal4* brain neurons (*R52B10-Gal4* × *tsh-Gal80*; *UAS-dTrpA1*, red circles or bars, $n = 16$) in DD. The behavior was monitored as described in Figure 2. Data are presented as mean ± SEM. $*p < 0.05$ vs. control; *t*-test. **(D,E)** Sleep profiles in 60-min intervals (D) or total daily sleep (E) for control flies (*R52B10-Gal4* × w^{1118}, black circles or bars, $n = 16$) or flies expressing *dTrpA1* in *R52B10-Gal4* except cholinergic neurons (*R52B10-Gal4* × *UAS-dTrpA1*; $Cha^{7.4kb}$-*Gal80*, red circles or bars, $n = 7$) in DD. Data are presented as mean ± SEM.

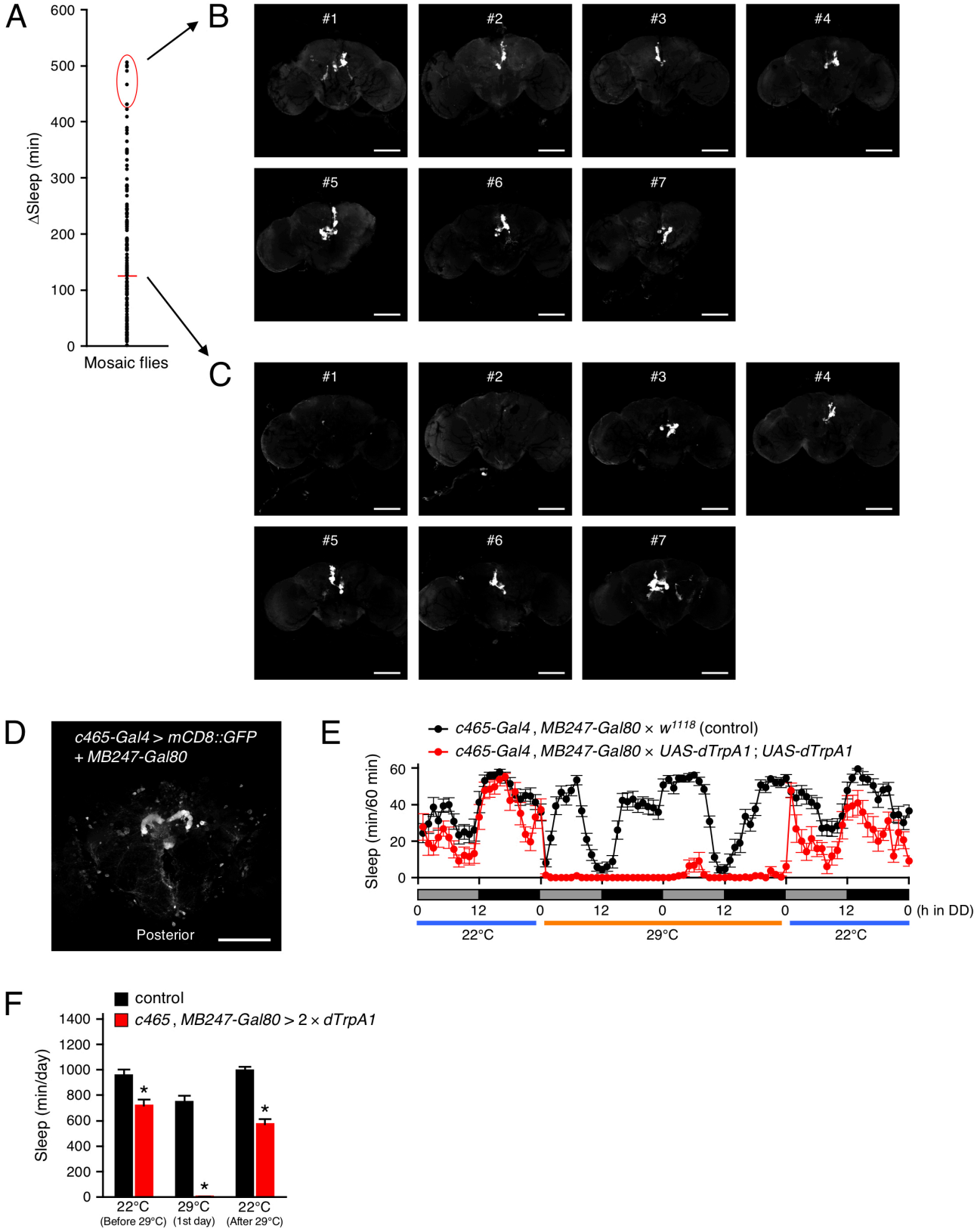

248 **Figure 5. *R52B10-Gal4*-expressing PFN neurons promote wakefulness.**

249 **(A)** Using the MARCM system, *dTrpA1* expression was targeted to a limited number of neurons in

250 *R52B10-Gal4*. The behavior of mosaic flies was monitored as described in Figure 2. Sleep change
251 (ΔSleep) of a single fly was calculated by subtracting the amount of sleep during the subjective night
252 at 29°C from that at 22°C (before 29°C) (n = 133). The red horizontal bar indicates the mean.
253 **(B,C)** Maximum-intensity projection of the confocal brain images of the flies whose ΔSleep were >
254 +2 SD higher than the mean (red oval in (A)) (B) or nearly equal to the mean (C). **(D)** Maximum-
255 intensity projection of the confocal brain images of *c465-Gal4*, *MB247-Gal80* crossed to *UAS-*
256 *mCD8::GFP* flies. *c465-Gal4* drives expression in the PFN neurons. **(E,F)** Sleep profiles in 60-
257 min intervals (E) or total daily sleep (F) for control (*c465-Gal4*, *MB247-Gal80* × w^{1118}, black circles
258 or bars, n = 15) or flies expressing *dTrpA1* in *c465-Gal4* except for mushroom body neurons (*c465-*
259 *Gal4*, *MB247-Gal80* × *UAS-dTrpA1*; *UAS-dTrpA1*, red circles or bars, n = 11) in DD conditions.
260 Behavior was monitored as described in Figure 2, except that flies were transferred to 29°C for 2 days
261 to allow dTrpA1 activation. Data are presented as mean ± SEM. *$p < 0.05$ vs. control; t-test. All
262 of the scale bars indicate 100 μm.

263 **The sleep-promoting PB interneurons had synaptic connections with the wake-promoting PFN**
264 **neurons**

265 To visualize putative dendritic and axonal terminals of the wake-promoting PFN neurons, both
266 DenMark (Nicolai et al., 2010), a specific somatodendritic marker and synaptotagmin (syt)-GFP
267 (Zhang et al., 2002), a presynaptic marker localized to synaptic vesicles were expressed using
268 *R52B10-Gal4*. These neurons displayed specific dendritic DenMark labeling in the PB and strong
269 labeling of presynaptic syt-GFP in the layer 1 of the FB and in the ventral NO (*Figure 6A*). In
270 addition, weak labeling of presynaptic terminals was also observed near the layers 2 to 3 of the FB
271 and in regions of the NO other than the ventral NO.

272 To assess synaptic connectivity between the sleep-promoting PB interneurons and the wake-
273 promoting PFN neurons, we employed a targeted GFP reconstitution across synaptic partners (t-
274 GRASP) technique (Shearin et al., 2018) under the control of two independent binary systems. A
275 part of the *cacophony* gene tagged with the *GFP11* fragment of a *split-GFP* (*pre-t-GRASP*), which is
276 targeted to axonal terminals and a portion of the mouse *Icam5* gene tagged with the *GFP1-10* (*post-*
277 *t-GRASP*), which is targeted to dendritic terminals were expressed by *R59E08-Gal4* and *R52B10-*
278 *LexA*, respectively. Reconstituted GFP signals were detected in the PB (*Figure 6B*), suggesting that
279 the sleep-promoting PB interneurons labeled by *R59E08-Gal4* have synaptic connections with the
280 wake-promoting PFN neurons marked by *R52B10-Gal4*.

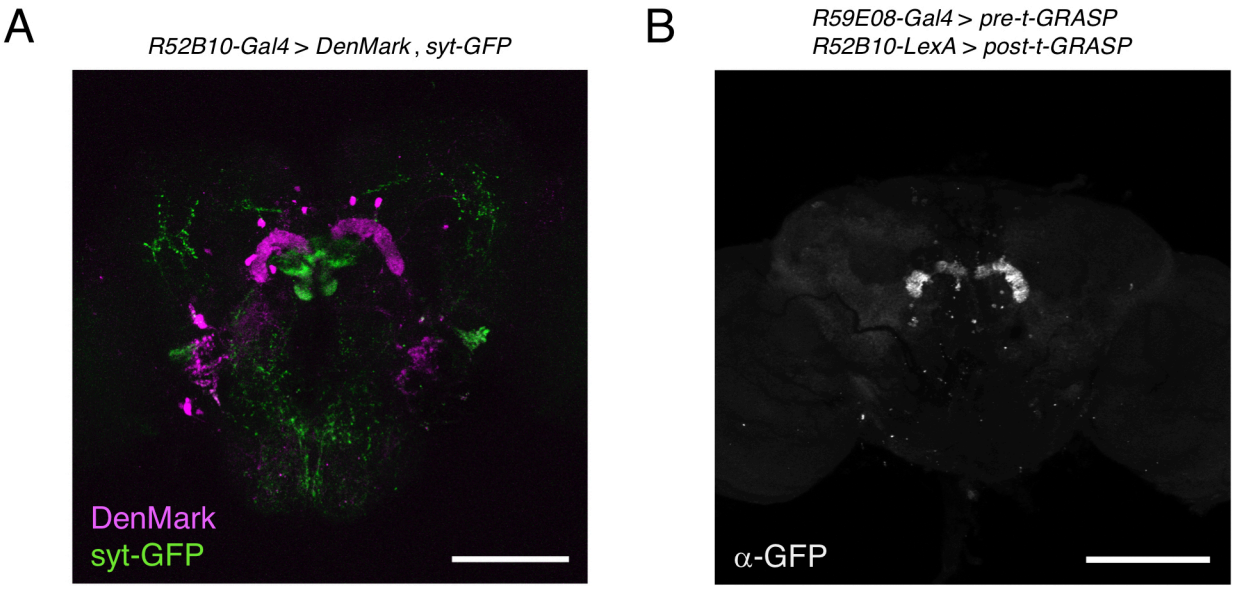

Figure 6. The sleep-promoting PB interneurons form synaptic contacts with the wake-promoting PFN neurons.

(A) The dendritic arbors and presynaptic terminals of the PFN neurons in *R52B10-Gal4* were visualized by expression of the postsynaptic marker DenMark and the presynaptic marker syt-GFP, respectively. **(B)** The neuronal connection of the sleep-promoting PB interneurons to the wake-promoting PFN neurons was revealed using the t-GRASP method. The *pre-t-GRASP* and the *post-t-GRASP* encode the split-GFP fragments, which are targeted to presynaptic endings and dendritic terminals, respectively. Brains expressing *pre-t-GRASP* with *R59E08-Gal4* and *post-t-GRASP* with *R52B10-LexA* were stained with a reconstituted GFP-specific antibody. The scale bars represent 100 μm.

291 **Dopamine signaling acted on the sleep-promoting PB interneurons for sleep regulation**

292 Dopamine has been identified as a key neurotransmitter in the regulation of sleep in *Drosophila*
293 (Andretic et al., 2005; Kume et al., 2005; Pimentel et al., 2016). In the *Drosophila* brain, DA
294 neurons are distributed in clusters, and each cluster is involved in various physiological phenomena,
295 including sleep-wake (Liu et al., 2012; Ueno et al., 2012; Sitaraman et al., 2015b). A pair of DA
296 neurons, named T1, has been previously observed with dendrites arborizing in the tritocerebrum and
297 with axons projecting to the PB (Nässel and Elekes, 1992; Alekseyenko et al., 2013). The
298 intersectional method combining the enhancer-trap flippase (FLP) transgenic line, FLP^{243} with a DA-
299 neuron specific *TH-Gal4* driver allows for the selective targeting of the T1 neurons (*Figure 7A*)
300 (Alekseyenko et al., 2013). Both activation and inhibition of the T1 DA neurons using this
301 intersectional method have been reported to specifically facilitate inter-male aggression. On the
302 other hand, inactivation of these neurons has no effect on locomotor activity and sleep amount
303 (Alekseyenko et al., 2013). We conditionally activated the T1 neurons with dTrpA1 and found that
304 the manipulation resulted in a significant decrease in the amount of sleep (*Figure 7B,C*).

305 Next, we examined whether T1 DA neurons directly connect with sleep-wake regulating PB
306 neurons by GRASP analysis utilizing membrane-tethered two complementary split-GFP fragments
307 (CD4-spGFP1-10 and CD4-spGFP11) (Feinberg et al., 2008). *TH-Gal4* was used to express *UAS-*
308 *CD4-spGFP1-10* and *R59E08-LexA* or *R52B10-lexA* were employed to drive *lexAop-CD4-spGFP11*,
309 respectively. Immunohistochemical signals for reconstituted GFP in the PB were detected only in
310 the combination of *TH-Gal4* and *R59E08-LexA* (*Figure 7D,E*). These signals were dot-like and
311 localized to the bilateral bends of the PB.

312 Alekseyenko and colleagues also demonstrate that Dopamine 2-like receptors (Dop2R also
313 known as D2R or DD2R), a functional counterpart of mammalian D2 receptor, are expressed in the
314 PB but not localized to the presynaptic terminals of T1 neurons. *Dop2R* knockdown using two
315 independent RNAi lines in the *R59E08-Gal4* expressing PB neurons resulted in a significant increase
316 in the amount of sleep compared to controls (*Figure 7F* and *Figure 7-figure supplement 1*). These
317 results support the idea that T1 DA neurons regulate sleep by acting on the sleep-promoting PB
318 interneurons via D2 receptor signaling.

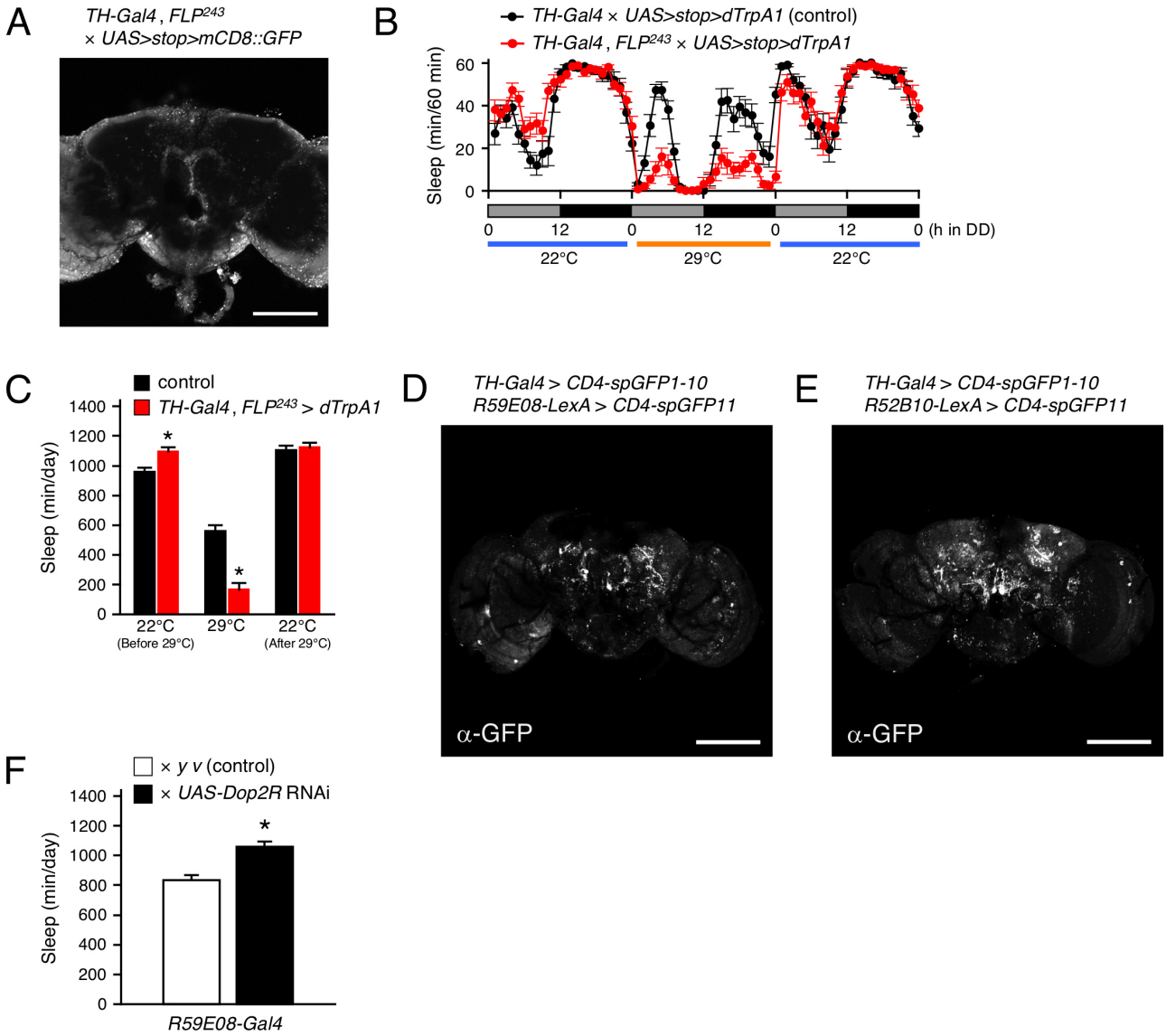

Figure 7. Dopamine regulates sleep by acting on the sleep-promoting PB interneurons. **(A)** Maximum-intensity projection of the confocal brain images of *TH-Gal4*, *FLP*^{243} crossed to *UAS>stop>mCD8::GFP* flies. *TH-Gal4*, *FLP*^{243} restricts expression to the T1 dopaminergic (DA) neurons that project to the PB. **(B,C)** Sleep profiles in 60-min intervals (B) or total daily sleep (C) for control (*TH-Gal4* × *UAS>stop>dTrpA1*, black circles or bars, $n = 15$) or flies expressing *dTrpA1* in T1 DA neurons (*TH-Gal4*, *FLP*^{243} × *UAS>stop>dTrpA1*, red circles or bars, $n = 16$) in DD conditions. The behavior was monitored as described in Figure 2. Data are presented as mean ± SEM. $*p < 0.05$ vs. control; *t*-test. **(D,E)** The anatomical connection of DA neurons in *TH-Gal4* to the sleep-promoting PB interneurons (D) or the wake-promoting PFN neurons (E) were examined using the GRASP method. Brains were stained with a reconstituted GFP-specific antibody. **(F)** Total daily sleep for control (white bar, $n = 15$) and *Dop2R* RNAi-expressing flies using the *R59E08-Gal4* driver (black bars, $n = 16$) in DD conditions. Data are averaged for 3 days and are presented as mean ± SEM. $*p < 0.05$; *t*-test. All of the scale bars indicate 100 μm.

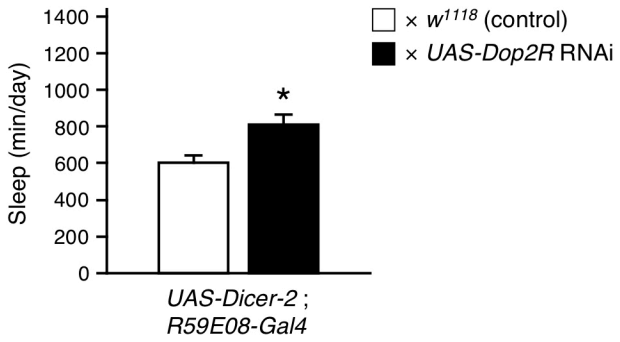

332 **Figure 7-figure supplement 1. *Dop2R* knockdown with *R59E08-Gal4* increased sleep.**
333 Total daily sleep for control (*UAS-Dicer-2*; *R59E08-Gal4* × w^{1118}, white bar, $n = 13$) and *Dop2R* RNAi
334 (VDRC 1820)-expressing flies using the *R59E08-Gal4* driver (*UAS-Dicer-2*; *R59E08-Gal4* × *UAS-*
335 *Dop2R* RNAi, black bars, $n = 13$) in DD conditions. Data are averaged for 3 days and are presented
336 as mean ± SEM. *$p < 0.05$; *t*-test.

337 **Discussion**

338 The data presented provide evidence that *Drosophila* sleep is controlled by the neuronal circuit in PB
339 consisting of the wake-promoting PFN neurons and the sleep-promoting PB interneurons and by the
340 T1-PB dopamine pathway (*Figure 7-figure supplement 2*). Previous anatomical,
341 electrophysiological and genetic studies have revealed the physiological functions of the PB in
342 several insect species. For example, in desert locusts, different types of PB neurons generate a
343 topographical map of the sky polarization pattern underlying sun compass orientation (Homberg et
344 al., 2011). Morphological counterparts of these locust's PB neurons are found in migratory monarch
345 butterflies and serve similar functions in processing polarized-light information (Heinze and Reppert,
346 2011). Experiments in fruit flies have demonstrated a role for the PB in locomotor control such as
347 walking speed, leg coordination, maintenance of walking activity, locomotor handedness and visual
348 targeting in gap-crossing behavior (Strauss et al., 1992; Strauss and Heisenberg, 1993; Martin et al.,
349 1999; Triphan et al., 2010; Buchanan et al., 2015). The locomotor activity of nob^{KS49} mutants has
350 been reported to be decreased compared to control flies but was increased in the present study (Martin
351 et al., 1999) (*Figure 1A*). We and Martin et al. assessed the number of activity counts per day or at
352 a particular time of day (4.5 hours) in nob^{KS49} flies as total locomotor activity, respectively. This
353 difference in assessment methods may have caused the phenotypic discrepancy in locomotor activity.
354 nob^{KS49} flies with a large gap at the sagittal midplane in the PB showed a significant reduction in the
355 amount of sleep (*Figure 1B*), suggesting a physical impairment of sleep-promoting neurons in this
356 mutant. We found that *R59E08-Gal4*-expressing PB interneurons promote sleep (*Figure 2* and
357 *Figure 3*). Analysis of single PB neurons labeled by MARCM or multicolor flip-out technique has
358 shown that PB interneurons are classified into three cell types based on their pattern of glomerular
359 innervation in the PB (Lin et al., 2013; Wolff et al., 2015). Two of the three cell types of PB
360 interneurons innervate all glomeruli, including the central part of the PB. Because the sleep-
361 promoting *R59E08-Gal4* was expressed throughout the PB, at least one of these two cell types of PB
362 interneurons would have been labeled with this driver. Although the cell type of PB interneurons
363 that promote sleep has been unidentified in our results, the two cell types may be physically damaged
364 in nob^{KS49} mutants.

365 Our MARCM experiment using *R52B10-Gal4* suggested that distinct types of PFN neurons
366 promote wakefulness (*Figure 5B*). There are five cell types of PFN neurons, which are PB output
367 neurons, classified according to their patterns of projection to the FB and the NO (Wolff et al., 2015).

368 Each PFN neuron belonging to the same cell type is further classified into subtypes that have different
369 patterns of arborization in the PB and arborize to one of the PB glomeruli. The *Gal4* line *c465*
370 drives expression in the wake-promoting PFN neurons (*Figure 5D-F*) (Lin et al., 2013; Buchanan et
371 al., 2015). Of the five cell types of PFN neurons, three are commonly labeled by *R52B10-Gal4* and
372 *c465-Gal4*, especially the cell type with axon terminals in layer 2 of the FB and in the ventral NO
373 exhibits high *Gal4* expression in these two drivers (Buchanan et al., 2015). On the other hand,
374 neuronal activation with *R44B10-Gal4*, which is highly expressed in all three cell types of PFN
375 neurons (Buchanan et al., 2015), was less effective in reducing the amount of sleep than neuronal
376 activation with *R52B10-Gal4* or *c465-Gal4* (*Figure 2A*). Although *R52B10-Gal4*, *c465-Gal4* and
377 *R44B10-Gal4* label the same cell types of PFN neurons, it is possible that the subtypes of PFN
378 neurons arborizing in one specific PB glomerulus which are co-labeled with *R52B10-Gal4* and *c465-*
379 *Gal4* are implicated in promoting arousal.
380 The t-GRASP experiment using *R59E08-Gal4* and *R52B10-LexA* suggested the sleep-
381 promoting PB interneurons form synaptic contacts with the wake-promoting PFN neurons (*Figure*
382 *6B*). The symmetrical patterns of the t-GRASP signal intensity in PB glomeruli should indicate
383 that this signal is not non-specific, supporting the idea described above that particular subtypes of
384 PFN neurons promote arousal. Sleep phenotypes of the flies in which *R59E08-Gal4*- or *R52B10-*
385 *Gal4*-expressing neurons were acutely activated, and axon-dendrite connectivity between these
386 sleep-regulating neurons suggest that the sleep-promoting PB interneurons inhibit the activity of the
387 wake-promoting PFN neurons. Because the sleep-promoting PB interneurons were predominantly
388 cholinergic (*Figure 3E,F*), the wake-promoting PFN neurons were likely to be regulated by
389 inhibitory acetylcholine receptor signaling (Ren et al., 2015). Functional connectivity analysis of
390 the central complex using Ca^{2+} imaging combined with optogenetics has demonstrated that
391 activation of one cell type of PB interneurons designated as Δ7 triggers the inhibitory response of
392 one cell type of PFN neurons (Franconville et al., 2018). However, since the Δ7 neurons are either
393 glutamatergic or GABAergic, they must not be the major PB interneurons to promote sleep.
394 Further anatomical and functional dissection of the sleep-regulating neuronal circuits in the PB
395 archived with promising *split-Gal4* lines will be required.
396 Previous studies have elucidated the control of *Drosophila* sleep by several clusters of DA
397 neurons (Liu et al., 2012; Ueno et al., 2012; Sitaraman et al., 2015b). This study revealed that the
398 PB-projecting T1 DA neurons physically connected to the sleep-promoting PB interneurons promote
399 wakefulness (*Figure 7A-D*). Because knockdown of *Dop2R* encoding Gi protein-coupled dopamine

400 receptor in *R59E08-Gal4*-expressing neurons significantly increased the amount of sleep (*Figure 7F*
401 and *Figure 7-figure supplement 1*), the simplest explanation is that dopamine inhibits the sleep-
402 promoting PB interneurons and thus promotes wakefulness. *Dop2R* null mutants have an increased
403 amount of sleep (Deng et al., 2019). The DopR2 function in the pars intercerebralis (PI) neurons
404 expressing Dilp2 and SIFamide has been shown to contribute to this sleep-increasing phenotype.
405 Our results show that, in addition to the PI, Dop2R also functions in the PB to regulate sleep.
406 T1 neurons were originally identified as neurons that specifically modulate aggression between
407 pairs of males (Alekseyenko et al., 2013). Regarding the interaction between sleep and aggression,
408 it has been shown that aggressive behaviors are suppressed in sleep-deprived male flies, and the
409 changes are mediated by octopamine signaling (Kayser et al., 2015). Interestingly, Duhart and
410 colleagues have recently reported that T1 neurons act downstream of courtship- and sleep-regulating
411 P1 neurons to modulate nutrition-dependent sleep-courtship balance in male flies (Duhart et al., 2020).
412 Elucidation of the mechanisms controlling the activity of T1 neurons may provide a novel link
413 between sleep, aggression and courtship.
414 More recently, we have successfully demonstrated that the wake-promoting PFN neurons
415 directly activate the FB interneurons (also known as pontine neurons) that appear to transmit
416 inhibitory acetylcholine signals to the sleep-promoting dFB neurons (Kato YS et al., unpublished
417 results, *Figure 7-figure supplement 2*). Further studies are required to determine the cellular and
418 molecular details of how these PB-dFB circuits control sleep-wakefulness.

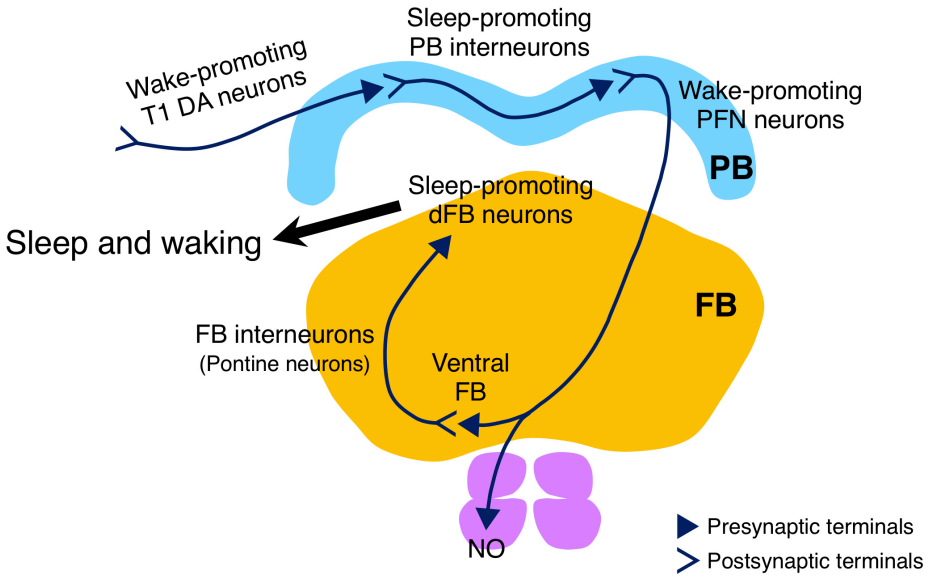

419 **Figure 7-figure supplement 2. Schematic drawing of the sleep-regulating neuronal circuit in**
420 **the PB.**
421 The circuit consists of the sleep-promoting PB interneurons and the wake-promoting PFN neurons,
422 and is regulated by the wake-promoting T1 DA neurons. The wake-promoting PFN neurons
423 indirectly inhibit the sleep-promoting dFB neurons via the FB interneurons (Kato YS et al.,
424 unpublished results).

Acknowledgments

We thank Drs. Roland Strauss, Paul A. Garrity, Julie H. Simpson, Takaomi Sakai, J. Douglas Armstrong, Edward A. Kravitz and Barry J. Dickson, the Bloomington *Drosophila* Stock Center, the Vienna *Drosophila* RNAi Center and the Kyoto Stock Center for providing fly lines used in this study. In addition, we also thank Dr. Taro Ueno (Toho University) and members of the Kume lab for helpful discussions. This work was supported by Japan Society for the Promotion of Science (JSPS) KAKENHI Grant Numbers JP18H02481, K.K., JP26507008, JP17K08571, J.T.

Competing interests

The authors declare that no competing interests exist.

Materials and Methods

Fly strains and rearing conditions

Fruit flies (*Drosophila melanogaster*) were raised at 25ºC in 50-60% relative humidity on standard medium containing cornmeal, yeast, glucose, wheat germ and agar. They were maintained under a 12-h light:12-h dark (LD) cycle. Eleven mutant flies with structural defects in the central complex *agnostic*^{X1} (*agn*^{X1}), *central-body-defect*^{KS171} (*cbd*^{KS171}), *cbd*^{KS188}, *cbd*^{762}, *central-complex-broad*^{KS145} (*ccb*^{KS145}), *central-complex-deranged*^{KS135} (*ccd*^{KS135}), *central-complex*^{KS181} (*cex*^{KS181}), *ellipsoid-body-open*^{KS263} (*ebo*^{KS263}), *ebo*^{678}, *ebo*^{1041} and *no-bridge*^{KS49} (*nob*^{KS49}) were kindly provided by Roland Strauss. *UAS-dTrpA1* lines on the second or third chromosomes were gifts from Paul A. Garrity and backcrossed over five generations to the control strain (*w*^{1118}). *teashirt* (*tsh*)-*Gal80*/CyO (Clyne and Miesenböck, 2008) was a gift from Julie H. Simpson. *Cha*$^{7.4kb}$-*Gal80* (Sakai et al., 2009) and *MB247-Gal80* (Krashes et al., 2007) were gifts from Takaomi Sakai. *c465-Gal4* (Young and Armstrong, 2010) was a gift from J. Douglas Armstrong. *FLP*^{243} (Alekseyenko et al., 2013) was a gift from Edward A. Kravitz. *UAS>stop>mCD8::GFP* (Yu et al., 2010) and *UAS>stop>dTrpA1* (von Philipsborn et al., 2011) were gifts from Barry J. Dickson. *R14F09-Gal4* (stock number: 48652), *R15E12-Gal4* (#48608), *R16D01-Gal4* (#48722), *R37G05-Gal4* (#48133), *R38G07-Gal4* (#50019), *R40A01-Gal4* (#50072), *R44B10-Gal4* (#50202), *R45G06-Gal4* (#50244), *R52B10-Gal4* (#38820), *R52G12-Gal4* (#49581), *R52H12-Gal4* (#38856), *R55G08-Gal4* (#50422), *R59A12-Gal4* (#39206), *R59E08-Gal4* (#39219), *R67B06-Gal4* (#48294), *R74C08-Gal4* (#46711) *R83A10-Gal4* (#48371), *R83H12-Gal4* (#40374), *R91A12-Gal4* (#40573), *10×UAS-IVS-mCD8::GFP* (#32187), *10×UAS-IVS-mCD8::GFP* (#32188), *UAS-DenMark*, *UAS-syt.eGFP* (#33064), *R52B10-LexA* (#52826), *R59E08-LexA* (#52832), *13×LexAop2-post-t-GRASP*, *20×UAS-pre-t-GRASP* (#79040), *UAS-CD4-spGFP1-10*, *lexAop-CD4-spGFP11* (#58755), *UAS-Dop2R-RNAi* (#50621) and *y*, *v*; *P{CaryP}attP40* (control line for TRiP RNAi lines, #36304) were obtained from the Bloomington *Drosophila* Stock Center, Indiana University, Indiana, USA. *UAS-Dop2R-RNAi* (VDRC ID: 1820), *UAS-Dicer-2* (60008) and *w*^{1118} (the genetic background for VDRC RNAi lines, 60000) were from the Vienna *Drosophila* RNAi Center (VDRC). *P{neoFRT}19A* (stock number: 106482) and *P{neoFRT}19A*, *tubP-GAL80*, *hsFLP*; *Pin*^{Yt}/CyO (#108064) were from the Kyoto Stock Center, Kyoto Institute of Technology, Kyoto, Japan.

Locomotor activity and sleep analysis

467 Locomotor activity of individual fly was measured using the *Drosophila* activity monitoring system
468 (TriKinetics, Waltham, MA) as described previously. Flies were placed individually in glass tubes
469 (length, 65 mm; inside diameter, 3 mm) containing either standard medium or sucrose-agar medium
470 (5% sucrose and 1% agar) at one end and were entrained for at least 3 days to LD cycles before
471 transferring to constant dark (DD) conditions. Two- to four-day-old male flies were used except for
472 MARCM experiments. Activity data were recorded continuously at 1-min intervals under both LD
473 and DD conditions. *Drosophila* sleep was defined as continuous immobile periods lasting 5 min or
474 longer based on previous reports (Hendricks et al., 2000; Shaw et al., 2000; Huber et al., 2004; Kume
475 et al., 2005). Total activity counts, total amount of sleep and waking activity index were analyzed
476 by Microsoft Excel-based software as previously described (Kume et al., 2005) and averaged over 3
477 days. For conditional dTrpA1 activation experiments, control and experimental flies were grown at
478 22ºC. Sleep measurements were performed in DD following LD cycles. At circadian time (CT) 0
479 (the beginning of a subjective day), temperature was raised from 22ºC to 29ºC for 24 h or 48 h to
480 activate dTrpA1-expressing neurons and then returned to 22ºC.
481
482 **Video tracking of locomotion**
483 Offspring from the control (*R59E08-Gal4* × *tsh-Gal80*) and the experimental (*R59E08-Gal4* × *tsh-*
484 *Gal80*; *UAS-dTrpA1*) crosses were housed in glass tubes and entrained to an LD cycle at 22ºC. After
485 entrainment, these flies were maintained in DD with illumination by near-infrared LEDs. At CT 0
486 on day 2 in DD, flies were transferred from 22ºC to 29ºC for 12 h to activate dTrpA1. The behavior
487 of flies was recorded at 2 frames/sec using a USB camera (Flea3 USB3.0: FL3-U3-13Y3M-C, Point
488 Grey Research Inc., Richmond, BC, Canada) fitted with a macro zoom lens (MLH-10X, computer,
489 Tokyo, Japan) during late subjective day (CT 8 to CT 12) at 29ºC. The captured images were
490 converted into 8-bit grayscale images. A composite background image was subtracted from each
491 video image. The position of individual fly was calculated for each subtracted image using the
492 Particle Tracker 2D/3D, an ImageJ plugin (Sbalzarini and Koumoutsakos, 2005).
493
494 **The MARCM system**
495 To generate flies for MARCM, female flies carrying *FRT19A*, *tub-GAL80*, *hs-FLP*; *UAS-dTrpA1* (X ;
496 II) crossed to males carrying *FRT19A*; *R52B10-Gal4*, *10×UAS-IVS-mCD8::GFP* (X ; III) at 22ºC.
497 Following egg-laying for 48 h, embryos or first instar larvae were heat-shocked at 37ºC for 1 h to
498 induce FLP-mediated recombination across two FRT sites. The amount of sleep in mosaic female

499 flies was measured at 22ºC and 29ºC under DD conditions. After sleep analysis, GFP expression
500 co-expressed with dTrpA1 in the brains was immunohistochemically determined.
501
502 **Immunohistochemistry**
503 To detect GFP expression in the MARCM experiments and reconstituted GFP signals in the t-GRASP
504 and GRASP experiments, whole-mount immunofluorescence staining of adult brains was performed
505 as described (Wu and Luo, 2006). For determination of GFP expression, GFP polyclonal antibody
506 (A6455, Thermo Fisher Scientific) was used at 1:250 dilution and goat anti-rabbit IgG, Alexa Fluor
507 568 (A11036, Thermo Fisher Scientific) was used at 1:200 dilution as secondary antibodies. We
508 used GFP recombinant rabbit monoclonal antibody (G10362, Thermo Fisher Scientific) at 1:300
509 dilution and monoclonal anti-GFP, clone GFP-20 (G6539, Sigma-Aldrich) at 1:100 dilution for
510 detection of reconstituted GFP signals in t-GRASP and GRASP experiments, respectively. Alexa
511 Fluor 488, goat anti-rabbit IgG (A11008, Thermo Fisher Scientific) and goat anti-mouse IgG (A11001,
512 Thermo Fisher Scientific) were used at 1:200 dilution as secondary antibodies.
513
514 **Confocal imaging**
515 Immunostained brain tissues were imaged by laser scanning confocal microscopes Zeiss LSM 510 or
516 LSM 800 (Carl Zeiss). Adult brains and ventral nerve cords expressing *mCD8::GFP* or *syt-GFP*
517 under the control of Gal4 were dissected and scanned by the confocal microscopes without staining.
518 In Figure 3A and Figure 4A, to examine the inhibitory effect of *tsh-Gal80* on the Gal4 activity of
519 *R59E08-Gal4* and *R52B10-Gal4*, the Gal4-driven *mCD8::GFP* expression in the brains or the ventral
520 nerve cords in the presence and absence of *tsh-Gal80* were imaged and processed in parallel using
521 identical settings on a confocal microscope.
522
523 **Statistical analysis**
524 Data were analyzed as described in the figure legends using Microsoft Excel and R: a language and
525 environment for statistical computing (R Core Team, 2020, https://www.R-project.org/).

526 **References**

527 Alekseyenko, O. V., Chan, Y.-B., Li, R., and Kravitz, E. A. (2013). Single dopaminergic neurons
528 that modulate aggression in Drosophila. *Proc. Natl. Acad. Sci. U. S. A.* 110, 6151–6.
529 doi:10.1073/pnas.1303446110.

530 Allada, R., and Siegel, J. M. (2008). Unearthing the phylogenetic roots of sleep. *Curr. Biol.* 18,
531 R670–R679. doi:10.1016/j.cub.2008.06.033.

532 Andretic, R., van Swinderen, B., and Greenspan, R. J. (2005). Dopaminergic modulation of arousal
533 in Drosophila. *Curr. Biol.* 15, 1165–75. doi:10.1016/j.cub.2005.05.025.

534 Buchanan, S. M., Kain, J. S., and de Bivort, B. L. (2015). Neuronal control of locomotor
535 handedness in Drosophila. *Proc. Natl. Acad. Sci.* 112, 6700–6705.
536 doi:10.1073/pnas.1500804112.

537 Campbell, S. S., and Tobler, I. (1984). Animal sleep: a review of sleep duration across phylogeny.
538 *Neurosci. Biobehav. Rev.* 8, 269–300. doi:10.1016/0149-7634(84)90054-x.

539 Cirelli, C., and Tononi, G. (2008). Is sleep essential? *PLoS Biol.* 6, e216.
540 doi:10.1371/journal.pbio.0060216.

541 Clyne, J. D., and Miesenböck, G. (2008). Sex-specific control and tuning of the pattern generator
542 for courtship song in Drosophila. *Cell* 133, 354–63. doi:10.1016/j.cell.2008.01.050.

543 Dag, U., Lei, Z., Le, J. Q., Wong, A., Bushey, D., and Keleman, K. (2019). Neuronal reactivation
544 during post-learning sleep consolidates long-term memory in Drosophila. *Elife* 8.
545 doi:10.7554/eLife.42786.

546 Deng, B., Li, Q., Liu, X., Cao, Y., Li, B., Qian, Y., et al. (2019). Chemoconnectomics: Mapping
547 Chemical Transmission in Drosophila. *Neuron* 101, 876-893.e4.
548 doi:10.1016/j.neuron.2019.01.045.

549 Donlea, J. M., Pimentel, D., and Miesenböck, G. (2014). Neuronal machinery of sleep homeostasis
550 in Drosophila. *Neuron* 81, 860–72. doi:10.1016/j.neuron.2013.12.013.

551 Donlea, J. M., Pimentel, D., Talbot, C. B., Kempf, A., Omoto, J. J., Hartenstein, V., et al. (2018).

552 Recurrent Circuitry for Balancing Sleep Need and Sleep. *Neuron* 97, 378-389.e4.
553 doi:10.1016/j.neuron.2017.12.016.

554 Donlea, J. M., Thimgan, M. S., Suzuki, Y., Gottschalk, L., and Shaw, P. J. (2011). Inducing sleep
555 by remote control facilitates memory consolidation in Drosophila. *Science* 332, 1571–6.
556 doi:10.1126/science.1202249.

557 Duhart, J. M., Baccini, V., Zhang, Y., Machado, D. R., and Koh, K. (2020). Modulation of sleep-
558 courtship balance by nutritional status in Drosophila. *Elife* 9. doi:10.7554/eLife.60853.

559 Feinberg, E. H., Vanhoven, M. K., Bendesky, A., Wang, G., Fetter, R. D., Shen, K., et al. (2008).
560 GFP Reconstitution Across Synaptic Partners (GRASP) defines cell contacts and synapses in
561 living nervous systems. *Neuron* 57, 353–63. doi:10.1016/j.neuron.2007.11.030.

562 Franconville, R., Beron, C., and Jayaraman, V. (2018). Building a functional connectome of the
563 drosophila central complex. *Elife*. doi:10.7554/eLife.37017.

564 Guo, F., Holla, M., Díaz, M. M., and Rosbash, M. (2018). A Circadian Output Circuit Controls
565 Sleep-Wake Arousal in Drosophila. *Neuron* 100, 624-635.e4.
566 doi:10.1016/j.neuron.2018.09.002.

567 Heinze, S., and Reppert, S. M. (2011). Sun compass integration of skylight cues in migratory
568 monarch butterflies. *Neuron* 69, 345–58. doi:10.1016/j.neuron.2010.12.025.

569 Hendricks, J. C., Finn, S. M., Panckeri, K. A., Chavkin, J., Williams, J. A., Sehgal, A., et al. (2000).
570 Rest in Drosophila is a sleep-like state. *Neuron* 25, 129–38. doi:10.1016/s0896-
571 6273(00)80877-6.

572 Homberg, U. (2008). Evolution of the central complex in the arthropod brain with respect to the
573 visual system. *Arthropod Struct. Dev.* 37, 347–62. doi:10.1016/j.asd.2008.01.008.

574 Homberg, U., Heinze, S., Pfeiffer, K., Kinoshita, M., and el Jundi, B. (2011). Central neural coding
575 of sky polarization in insects. *Philos. Trans. R. Soc. Lond. B. Biol. Sci.* 366, 680–7.
576 doi:10.1098/rstb.2010.0199.

577 Huber, R., Hill, S. L., Holladay, C., Biesiadecki, M., Tononi, G., and Cirelli, C. (2004). Sleep
578 homeostasis in Drosophila melanogaster. *Sleep* 27, 628–39. doi:10.1093/sleep/27.4.628.

579 Jenett, A., Rubin, G. M., Ngo, T.-T. B., Shepherd, D., Murphy, C., Dionne, H., et al. (2012). A
580 GAL4-Driver Line Resource for Drosophila Neurobiology. *Cell Rep.* 2, 991–1001.
581 doi:10.1016/j.celrep.2012.09.011.

582 Joiner, W. J., Crocker, A., White, B. H., and Sehgal, A. (2006). Sleep in Drosophila is regulated by
583 adult mushroom bodies. *Nature* 441, 757–760. doi:10.1038/nature04811.

584 Kayser, M. S., Mainwaring, B., Yue, Z., and Sehgal, A. (2015). Sleep deprivation suppresses
585 aggression in Drosophila. *Elife* 4. doi:10.7554/eLife.07643.

586 Krashes, M. J., Keene, A. C., Leung, B., Armstrong, J. D., and Waddell, S. (2007). Sequential use
587 of mushroom body neuron subsets during drosophila odor memory processing. *Neuron* 53,
588 103–15. doi:10.1016/j.neuron.2006.11.021.

589 Kume, K., Kume, S., Park, S. K., Hirsh, J., and Jackson, F. R. (2005). Dopamine is a regulator of
590 arousal in the fruit fly. *J. Neurosci.* 25, 7377–84. doi:10.1523/JNEUROSCI.2048-05.2005.

591 Lamaze, A., Krätschmer, P., Chen, K.-F., Lowe, S., and Jepson, J. E. C. (2018). A Wake-Promoting
592 Circadian Output Circuit in Drosophila. *Curr. Biol.* 28, 3098-3105.e3.
593 doi:10.1016/j.cub.2018.07.024.

594 Lin, C.-Y., Chuang, C.-C., Hua, T.-E., Chen, C.-C., Dickson, B. J., Greenspan, R. J., et al. (2013).
595 A comprehensive wiring diagram of the protocerebral bridge for visual information processing
596 in the Drosophila brain. *Cell Rep.* 3, 1739–53. doi:10.1016/j.celrep.2013.04.022.

597 Liu, Q., Liu, S., Kodama, L., Driscoll, M. R., and Wu, M. N. (2012). Two dopaminergic neurons
598 signal to the dorsal fan-shaped body to promote wakefulness in Drosophila. *Curr. Biol.* 22,
599 2114–23. doi:10.1016/j.cub.2012.09.008.

600 Liu, S., Liu, Q., Tabuchi, M., and Wu, M. N. (2016). Sleep Drive Is Encoded by Neural Plastic
601 Changes in a Dedicated Circuit. *Cell* 165, 1347–1360. doi:10.1016/j.cell.2016.04.013.

602 Martin, J. R., Raabe, T., and Heisenberg, M. (1999). Central complex substructures are required for
603 the maintenance of locomotor activity in Drosophila melanogaster. *J. Comp. Physiol. A.* 185,
604 277–88. doi:10.1007/s003590050387.

605 Nässel, D. R., and Elekes, K. (1992). Aminergic neurons in the brain of blowflies and Drosophila:

606 dopamine- and tyrosine hydroxylase-immunoreactive neurons and their relationship with
607 putative histaminergic neurons. *Cell Tissue Res.* doi:10.1007/BF00318701.

608 Ni, J. D., Gurav, A. S., Liu, W., Ogunmowo, T. H., Hackbart, H., Elsheikh, A., et al. (2019).
609 Differential regulation of the Drosophila sleep homeostat by circadian and arousal inputs. *Elife*
610 8. doi:10.7554/eLife.40487.

611 Nicolai, L. J. J., Ramaekers, A., Raemaekers, T., Drozdzecki, A., Mauss, A. S., Yan, J., et al.
612 (2010). Genetically encoded dendritic marker sheds light on neuronal connectivity in
613 Drosophila. *Proc. Natl. Acad. Sci.* 107, 20553–20558. doi:10.1073/pnas.1010198107.

614 Pimentel, D., Donlea, J. M., Talbot, C. B., Song, S. M., Thurston, A. J. F., and Miesenböck, G.
615 (2016). Operation of a homeostatic sleep switch. *Nature* 536, 333–337.
616 doi:10.1038/nature19055.

617 Pitman, J. L., McGill, J. J., Keegan, K. P., and Allada, R. (2006). A dynamic role for the mushroom
618 bodies in promoting sleep in Drosophila. *Nature* 441, 753–756. doi:10.1038/nature04739.

619 Ren, G. R., Folke, J., Hauser, F., Li, S., and Grimmelikhuijzen, C. J. P. (2015). The A- and B-type
620 muscarinic acetylcholine receptors from Drosophila melanogaster couple to different second
621 messenger pathways. *Biochem. Biophys. Res. Commun.* 462, 358–64.
622 doi:10.1016/j.bbrc.2015.04.141.

623 Sakai, T., Kasuya, J., Kitamoto, T., and Aigaki, T. (2009). The Drosophila TRPA channel, Painless,
624 regulates sexual receptivity in virgin females. *Genes. Brain. Behav.* 8, 546–57.
625 doi:10.1111/j.1601-183X.2009.00503.x.

626 Sbalzarini, I. F., and Koumoutsakos, P. (2005). Feature point tracking and trajectory analysis for
627 video imaging in cell biology. *J. Struct. Biol.* 151, 182–95. doi:10.1016/j.jsb.2005.06.002.

628 Shaw, P. J., Cirelli, C., Greenspan, R. J., and Tononi, G. (2000). Correlates of sleep and waking in
629 Drosophila melanogaster. *Science* 287, 1834–7. doi:10.1126/science.287.5459.1834.

630 Shearin, H. K., Quinn, C. D., Mackin, R. D., Macdonald, I. S., and Stowers, R. S. (2018). t-GRASP,
631 a targeted GRASP for assessing neuronal connectivity. *J. Neurosci. Methods* 306, 94–102.
632 doi:10.1016/j.jneumeth.2018.05.014.

633 Sitaraman, D., Aso, Y., Jin, X., Chen, N., Felix, M., Rubin, G. M., et al. (2015a). Propagation of
634 Homeostatic Sleep Signals by Segregated Synaptic Microcircuits of the Drosophila Mushroom
635 Body. *Curr. Biol.* 25, 2915–27. doi:10.1016/j.cub.2015.09.017.

636 Sitaraman, D., Aso, Y., Rubin, G. M., and Nitabach, M. N. (2015b). Control of Sleep by
637 Dopaminergic Inputs to the Drosophila Mushroom Body. *Front. Neural Circuits* 9, 73.
638 doi:10.3389/fncir.2015.00073.

639 Strauss, R., Hanesch, U., Kinkelin, M., Wolf, R., and Heisenberg, M. (1992). No-bridge of
640 Drosophila melanogaster: portrait of a structural brain mutant of the central complex. *J.*
641 *Neurogenet.* 8, 125–55. doi:10.3109/01677069209083444.

642 Strauss, R., and Heisenberg, M. (1993). A higher control center of locomotor behavior in the
643 Drosophila brain. *J. Neurosci.* 13, 1852–61. Available at:
644 http://www.ncbi.nlm.nih.gov/pubmed/8478679 [Accessed January 31, 2020].

645 Triphan, T., Poeck, B., Neuser, K., and Strauss, R. (2010). Visual targeting of motor actions in
646 climbing Drosophila. *Curr. Biol.* 20, 663–8. doi:10.1016/j.cub.2010.02.055.

647 Ueno, T., Tomita, J., Tanimoto, H., Endo, K., Ito, K., Kume, S., et al. (2012). Identification of a
648 dopamine pathway that regulates sleep and arousal in Drosophila. *Nat. Neurosci.* 15, 1516–
649 1523. Available at: http://www.nature.com/doifinder/10.1038/nn.3238.

650 von Philipsborn, A. C., Liu, T., Yu, J. Y., Masser, C., Bidaye, S. S., and Dickson, B. J. (2011).
651 Neuronal control of Drosophila courtship song. *Neuron* 69, 509–22.
652 doi:10.1016/j.neuron.2011.01.011.

653 Wolff, T., Iyer, N. A., and Rubin, G. M. (2015). Neuroarchitecture and neuroanatomy of the
654 Drosophila central complex: A GAL4-based dissection of protocerebral bridge neurons and
655 circuits. *J. Comp. Neurol.* doi:10.1002/cne.23705.

656 Wu, J. S., and Luo, L. (2006). A protocol for dissecting Drosophila melanogaster brains for live
657 imaging or immunostaining. *Nat. Protoc.* 1, 2110–2115. doi:10.1038/nprot.2006.336.

658 Young, J. M., and Armstrong, J. D. (2010). Structure of the adult central complex in Drosophila:
659 organization of distinct neuronal subsets. *J. Comp. Neurol.* 518, 1500–24.

660 doi:10.1002/cne.22284.

661 Yu, J. Y., Kanai, M. I., Demir, E., Jefferis, G. S. X. E., and Dickson, B. J. (2010). Cellular
662 organization of the neural circuit that drives Drosophila courtship behavior. *Curr. Biol.* 20,
663 1602–14. doi:10.1016/j.cub.2010.08.025.

664 Zhang, Y. Q., Rodesch, C. K., and Broadie, K. (2002). Living synaptic vesicle marker:
665 synaptotagmin-GFP. *Genesis* 34, 142–5. doi:10.1002/gene.10144.